Magazine of Civil Engineering

ISSN 2712-8172

journal homepage: http://engstroy.spbstu.ru/

Research article

UDC 681.7.035:552.55

DOI: 10.34910/MCE.116.15

Porous glass ceramics from siliceous rocks with high operating temperature

A.I. Rodin ✉ , ***A.A. Ermakov*** , ***V.M. Kyashkin*** , ***N.G. Rodina*** , ***V.T. Erofeev***

National Research Mordovia State University, Saransk, Republic of Mordovia, Russia

✉ *al_rodin@mail.ru*

Keywords: glass ceramic, construction material, thermal insulation, siliceous rocks, aluminium oxide, compressive strength, thermal conductivity, thermal analysis

Abstract. Porous glass-ceramic materials although light weighted have relatively high strength, low thermal and sound conductivity, high corrosion resistance, and are non-combustible, etc. They can be obtained from siliceous rocks, the reserves of which are huge. The article considers the obtaining of porous glass ceramic materials with an operating temperature exceeding 900 °C. The materials are obtained from siliceous rocks, Na_2CO_3, Al_2O_3 and KCl. Mechanochemical activation of raw materials was carried out in a planetary ball mill. The resulting charge mixture was annealed at a temperature of 850 °C. Experimental results were obtained by using X-ray diffraction (XRD) and thermal (TA) analysis, scanning electron microscopy (SEM), X-ray microtomography (Micro-CT). Physical-mechanical, thermophysical properties and chemical stability of obtained materials were examined. The main crystalline phase of glass ceramics from the calcite-free charge mixture is anorthoclase and quartz. Apart from that samples with calcite charge mixture contain wollastonite and devitrite. The increased content of Al_2O_3 in the charge mixture displays nepheline in glass ceramics. Calcite in the charge mixture has a significant effect on the microstructure of porous glass ceramics. The number of open pores in the material increases from ≈ 5 % to > 50 %. The compressive strength of porous glass-ceramic materials derived from siliceous rocks reaches 5.1 MPa. In terms of strength, they are significantly superior to foam glass. The minimum thermal conductivity of glass ceramics is 0.065 W/(m·°C) at a sample density of 244 kg/m^3. Samples withstand temperature drops by 230 °C. The material has a high chemical stability and can be operated at temperatures reaching 920 °C inclusively. The obtained materials can be used as thermal insulation of boiler equipment, melting furnaces, etc.

Acknowledgement: The study was funded by a grant Russian Science Foundation No. 21-79-10422, https://rscf.ru/project/21-79-10422/

Citation: Rodin, A.I., Ermakov, A.A., Kyashkin, V.M., Rodina, N.G., Erofeev, V.T. Porous glass ceramics from siliceous rocks with high operating temperature. Magazine of Civil Engineering. 2022. 116(8). Article no. 11615. DOI: 10.34910/MCE.116.15

1. Introduction

Porous glass-ceramic materials although light weighted have relatively high strength, low thermal and sound conductivity, high corrosion resistance, and are non-combustible, etc. [1, 2]. Porous glass ceramic is not inferior in many properties to other modern building materials [3–5]. They are highly sought for various purposes during the construction and repair of facilities. In civil engineering, this material can be used for mounting wall enclosing structures [6], insulation of facades, roofs, floors [7], in the decoration of structures [8], etc. The industry puts them to use in refractory lining of furnaces [2], for heat and sound insulation [9], protection of structures from corrosion [10], etc.

© Rodin, A.I., Ermakov, A.A., Kyashkin, V.M., Rodina, N.G., Erofeev, V.T., 2022. Published by Peter the Great St. Petersburg Polytechnic University.

Porous glass-ceramic materials are obtained from slags of various industries [11–13], glass waste [14], fly ash [1, 7, 15, 16] and other components. Many scholarly works consider the production of porous glass-ceramic materials from siliceous rocks [17–20]. The reserves of such rocks in the world are immense [17, 21]. Diatomite, zeolite-containing tripoli, opoka are activated with aqueous solutions of high concentrated NaOH, granulated, and then annealed. We have proposed a method for obtaining porous glass ceramics from zeolite-containing rocks. The method allows to obtain samples in the form of blocks [22]. The rock, together with sodium carbonate or thermonatrite, was exposed to mechanochemical activation in a planetary mill. The resulting charge mixture was put into the molds of the required size and then annealed [23]. When annealed, zeolite minerals in the charge mixture are dehydrated sealing surface hydroxyl groups in micropores. At a temperature of more than 670 °C, the charge mixture begins to melt. Hydroxyl groups condense, water vapor releases foaming the charge mixture [24]. The obtained materials have relatively high strength, low thermal conductivity. However, their limiting operating temperature does not exceed 850 °C [22, 23]. This is not enough for thermal insulation of many industrial facilities [2].

There is a great deal of research into the influence of glass ceramics' chemical and phase composition on its operating temperature. The limiting temperature of glass ceramics decreases following the increase in Fe_2O_3 and CaO added to its composition [13, 25, 26]. The influence of MgO on its properties is similar to that of CaO [27], but many siliceous rocks compositions have a low MgO content [17, 18, 23]. The resistance of ceramic materials derived from industrial waste or artificially created glass to a lasting exposure to high temperatures raises after the increase of Al_2O_3 in their composition [28, 29]. The technology of obtaining porous glass ceramics from siliceous rocks differs from those referred above. There are differences in the chemical and phase composition of materials [19, 23]. The increased content of amorphous SiO_2 in the siliceous charge mixture's composition decreases the limiting operating temperature of porous glass ceramics. Na_2O and Fe_2O_3 produce negative effect as well [23]. Research findings dealing with the effect of CaO and Al_2O_3 on the limiting operating temperature of porous glass ceramics from siliceous rocks have not been found.

The objective of research: to obtain porous glass-ceramic materials from siliceous rocks with an operating temperature of more than 900 °C in one stage of charge mixture heating; to study the structure and properties of the obtained materials.

Tasks:

- by utilizing the X-ray diffraction (XRD) and thermal (TA) analysis to determine the effect of calcite and aluminum oxide content in the charge mixture on its phase composition after mechanochemical activation, phase transformations in the charge mixture during heating and the phase composition of annealed porous glass ceramics;
- by employing scanning electron microscopy (SEM) and X-ray microtomography (Micro-CT) to study the microstructure of porous glass ceramics from siliceous rocks;
- to establish the influence of the phase composition of porous glass ceramic samples on their physical and mechanical properties (density, porosity, bending strength and compressive strength);
- to determine the thermophysical properties (thermal conductivity, thermal shock resistance, limiting operating temperature) of porous glass-ceramic material samples;
- to determine the chemical stability of the developed materials to water, aqueous solutions of acids and alkalis.

2. Methods

2.1. Materials

To fabricate samples of porous glass-ceramic materials the following components were used:

- Siliceous rocks: R1 is zeolite-containing tripoli (calcite content is 0%), R2 is zeolite-containing tripoli (calcite content is 10.5 %), R3 is diatomite. Humidity of raw materials components is less than 1 %. The chemical and mineralogical composition of the rocks is shown in Table 1 and 2, respectively.

Table 1. Chemical composition.

Composition No.	Chemical composition (wt.%)							
	SiO_2	CaO	Al_2O_3	Fe_2O_3	K_2O	MgO	TiO_2	Na_2O
1	2	3	4	5	6	7	8	9
R1 (Tripoli)	70.94	2.38	12.38	3.52	1.71	1.66	0.50	0.14
R2 (Tripoli)	67.86	7.74	7.61	1.99	1.56	1.07	0.34	0.17
R3 (Diatomite)	81.47	1.51	5.34	2.05	0.97	0.89	0.25	0.20

Continuation of table

Chemical composition, (wt.%)									
SO_3	P_2O_5	ZrO_2	MnO	Cr_2O_3	NiO	SrO	BaO	V_2O_5	LOI
10	11	12	13	14	15	16	17	18	19
0.02	0.26	0.02	0.01	0.01	0.01	0.06	0.00	0.01	6.37
0.06	0.15	0.01	0.01	0.01	0.00	0.06	0.02	0.01	11.32
1.77	0.03	0.01	0.01	0.01	0.00	0.01	0.02	0.01	5.45

Table 2. Mineralogical composition of rocks.

Composition No.	Mineralogical composition, %					
	Quartz	Calcite	Heulandite	Muscovite	Cristobalite	Amorphous phase
R1	29.1	0.0	18.6	16.1	16.2	20.0
R2	15.5	10.5	20.4	13.1	20.5	20.0
R3	10.9	0.0	0.0	8.1	0.0	80.0

- Sodium carbonate. Chemical formula: Na_2CO_3. The purity is ≥ 99 %. The additive was introduced to reduce the melting temperature and foaming of the charge mixture. The required concentration of the additive was determined by us earlier [22].
- Aluminum Oxide. Chemical formula: Al_2O_3. The purity is ≥ 97 %. The additive was introduced to increase the limiting operating temperature of porous glass-ceramic materials. Theoretical assumptions on increasing the operating temperature of glass ceramics owing to the introduction of Al_2O_3 are described in the Introduction.
- Potassium chloride. Chemical formula: KCl. The purity is ≥ 99 %. The addition of KCl is necessary to obtain a uniform pore structure in glass ceramics. The required concentration of the additive was determined by us in earlier works [22].

2.2. Compositions and fabrication of samples

The charge mixture for porous glass-ceramic samples was obtained by joint grinding (mechanochemical activation) of siliceous rocks, sodium carbonate, aluminum oxide and potassium chloride. The raw materials were ground in a planetary ball mill Retsch PM 400. Grinding time – 35 min. The overload inside the crushing cylinder is 20G. The resulting charge mixture was annealed in a metal form in a muffle furnace. The internal size of the mold is 120×120×260 mm. Before annealing, the molds were coated with clay. Annealing procedure: heating to 670 °C at a speed of 4.5 °C/min, holding at 670 °C – 1 hour, heating to the temperature of 850 °C at a speed of 4.5 °C/min, holding at 850 °C – 30 minutes. The holding at 670 °C is necessary to complete the decomposition of select minerals of the charge mixture (calcite, muscovite). If this stage is excluded from the technological cycle, samples of porous glass ceramics will have an uneven macrostructure. Holding at 850 °C is necessary for the completion of all phase formation processes [22]. The molds with the resulting material after annealing cooled down together with the furnace to 40 °C. Then the forms were disassembled. The samples were sawed and tested. The diagram of the experiment is shown in Fig. 1.

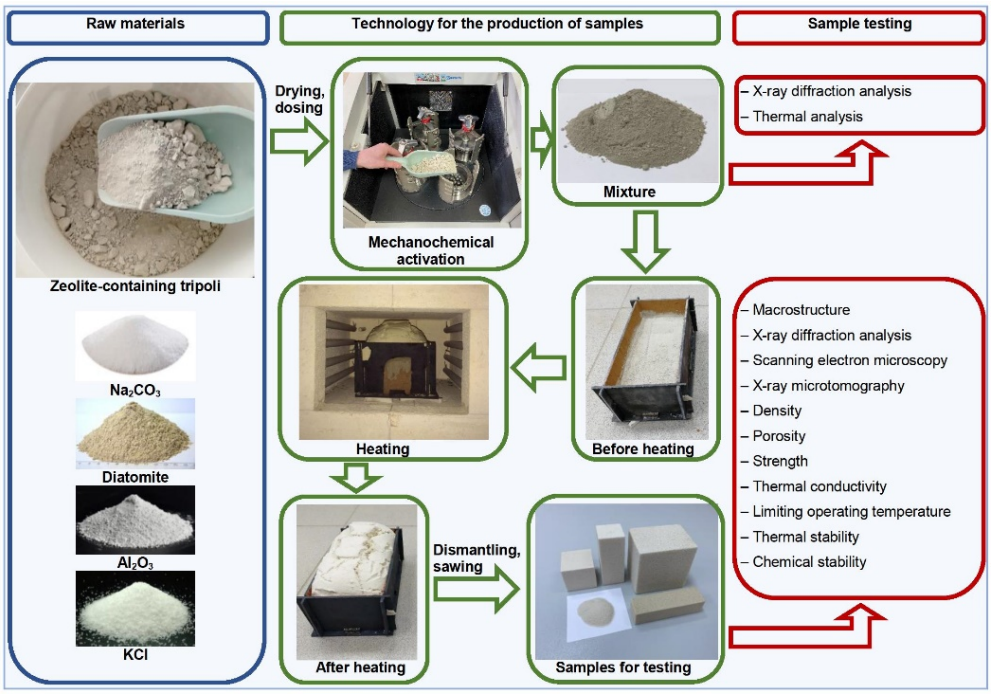

Figure 1. Diagram of the experiment.

In the course of experiment, 16 charge mixture compositions were tested. The compositions are presented in Table 3.

Table 3. Compositions, examined in work.

Composition No.	Charge mixture composition, %					
	Siliceous rock (chemical composition see Table 1)			Al_2O_3	Na_2CO_3	KCl
	R1	R2	R3			
C1	81.4	0	0	0	18.4	0.2
C2	80.38	0	0	1.02		
C3	79.36	0	0	2.04		
C4	78.35	0	0	3.05		
C5	52.73	25.97	2.70	0		
C6	51.36	25.30	2.70	2.04		
C7	50	24.63	2.70	4.07		
C8	48.63	23.96	2.70	6.11		
C9	25.07	50.90	5.43	0		
C10	24.06	48.86	5.43	3.05		
C11	23.05	46.81	5.43	6.11		
C12	22.05	44.76	5.43	9.16		
C13	0	73.26	8.14	0		
C14	0	69.19	8.14	4.07		
C15	0	65.12	8.14	8.14		
C16	0	61.05	8.14	12.21		

2.3. Analytical techniques

Methods for obtaining experimental data:

– X-ray diffraction analysis (XRD) of charge mixture samples and annealed materials was made by using the Empyrean PANalytic diffractometer (Netherlands). The samples were grinded to a fraction of less than 90 μm. Diffraction patterns were identified in CuK_a emission in the scan range 2Θ = 4–80°. The PIXcel3D semiconductor detector operated in linear scanning mode. The step size is 0.0067 °/min, the counting time is 150 seconds. The qualitative phase composition of the samples was determined by the Hanawalt method using the ICDD PDF-2 database.

- Thermal analysis (TA) of charge mixture samples was made by using the TGA/DSC1 apparatus (Switzerland). 20±0.1 mg of charge mixture was put into an 150-mcl. alumina crucible. By tapping the crucible on the table, the sample was compacted. The crucible with the charge mixture was then placed in the apparatus to be heated in the range between 30 and 850 °C at a rate of 10 °C/min.
- Scanning electron microscopy (SEM) of porous glass-ceramic samples was performed using the Quanta 200 3D device (USA). The samples were scanned at a pressure of 60 Pa, with an accelerating voltage of 30 kV and an operating distance of 15 mm.
- X-ray microtomography (Micro-CT) was made using the SkyScan 1172 apparatus (Belgium). Samples with a size of 15±1 mm were X-rayed at 67 kV and 110 mcA. The angle of rotation of the supporting post is 360°, the rotation pace is 0.6°. Images were collected with a resolution of 6.9 mcm. Images processed with CTvox software (Skyscan, Belgium).
- The true density of porous glass ceramic samples (ρ_0, g/cm^3) was determined using a pycnometer. The tests were effectuated on grinded (fraction < 20 μm) and dried samples. The arithmetic mean of the test results of two samples of each composition was taken as the result.
- Porosity (open, closed and total) was determined on cubic-form samples with a side plane size of 50±5 mm. First, the volume (V, cm^3) and the weight of dry samples (m_o, g) were determined. Then they were placed in a cylindrical tank with water for vacuuming. The water level in the cylindrical tank was at least 20 mm higher than the samples. The hydrometer was used to determine the water density (ρ_w, g/cm^3). The air was pumped out of the cylindrical tank. The residual pressure in the working chamber was 2,000 Pa. The samples were held in the vacuum for at least 2 hours. Testing samples were taken out of the tank after weight stabilisation. After water saturation, the samples weight was measured indoors (m_1, g).

The apparent density (ρ, g/cm^3) was calculated by the formula (1):

$$\rho = \frac{m_0}{V}. \quad (1)$$

Total porosity (P_t, %) was calculated by the formula (2):

$$P_t = \frac{\rho_0 - \rho}{\rho} \cdot 100. \quad (2)$$

Open porosity (P_o, %) was calculated by the formula (3):

$$P_o = \frac{m_1 - m_0}{V \cdot \rho_w} \cdot 100. \quad (3)$$

Closed porosity (P_c, %) was calculated by the formula (4):

$$P_c = P_t - P_o. \quad (4)$$

The arithmetic mean of the test results of three samples of each composition was taken as the final result.

- The compressive strength of porous glass-ceramic materials was determined on dry cubic samples with a side plane of 90±5 mm. The maximum destructive force was identified when the sample was fractured (cracks appeared) or deformed in the surface layers by 10 % of the initial height. The arithmetic mean of the test results of five samples of each composition was taken as the final result.
- The bending strength was determined on dry samples-beams with side plane sizes 120×30×30 mm. The sample was placed on two cylindrical supports with a diameter of 6±0.1 mm. The distance between the axes of the supports is 100±1 mm. The load on the sample was applied by a rod with a diameter of 6±0.1 mm. The rod was put along the entire width of the sample at an equal distance from the supports. The rate of application of the load is 5 mm/min. The load was identified at the moment of sample's destruction. The bending strength was determined according to the standard formula. The arithmetic mean of the test results of three samples of each composition was taken as the final result.

- The thermal conductivity of the material was determined by the probe method using the MTCM–1 apparatus (mobile thermal conductivity meter). The experiment was carried out on samples of cubic shape with a side plane of 90±5 mm. The samples were previously dried. A hole with a diameter of 6 mm and a depth of 50 to 60 mm was drilled in the center of the side plane. The apparatus (MTCM–1) and the prepared samples were kept for 2 days in the laboratory at a temperature of 22±1 °C. A probe with a diameter of 6 mm was immersed into the hole. Kept making readings of the apparatus. The arithmetic mean of the test results of five samples of each composition was taken as the final result.
- The thermal shock resistance (ΔT, °C) of the materials was revealed against the appearance of cracks on the samples during abrupt cooling. Dry samples of cubic shape (side plane length 50±5 mm) were kept in a thermostat at a temperature of 110 °C for at least 2 hours. Heated samples were quickly (< 10 seconds) removed from the thermostat and immersed in a water container (water temperature – 20±2°C). The samples were kept in water for 65±5 seconds. The experiment was repeated increasing the thermostat temperature by 10 °C until cracks appeared on all samples. The thermal shock resistance of each sample was calculated by the formula (5):

$$\Delta T = T_t - T_w - 10, \tag{5}$$

where T_t is the thermostat temperature at which the sample was kept (°C); T_w is water temperature in the container (°C); 10 is the thermostat temperature difference between the subsequent and previous tests (°C).

When determining the thermal shock resistance, the arithmetic mean of the test results of four samples of each composition was taken as the final result.

- The limiting operating temperature of porous glass-ceramic materials was estimated by the residual change in the size of the samples (90×40×40 mm) after heating. The samples were measured with an accuracy of 0.01 mm and put in a vertical position in a muffle furnace. The samples were heated in the furnace at a rate of 10° C/min to a temperature 50 °C less than the set temperature. To the limiting temperature heated at a rate of 2 °C/min. The samples were kept at a given temperature for 2 hours. If after the test the sample sizes changed by < 1 %, the experiment was repeated increasing in the limiting temperature by 10 °C. The arithmetic mean of the test results of three samples of each composition was taken as the final result
- The chemical stability of the materials was estimated by the mass loss of powdered samples after boiling in distilled water, an aqueous solution of 6N HCl, a mixture of equal volumes of 1N solutions of Na_2CO_3 and NaOH. Porous glass ceramic materials were grinded to a fraction of 0.315–0.630 mm. A dried sample weighing 5±0.0005 g was placed in a test jar and drenched with 100±0.5 cm^3 of reagent. The test jar was connected to a backflow condenser and boiled for 3 hours. After boiling, an aggressive liquid was discharged. The sample was washed with distilled water. The washed sample was drained through a funnel with a paper ash-free filter. The filter with the sample was placed in a quartz crucible and annealed (1 hour) in a muffle furnace at a temperature of 800±10 °C. The crucible with the sample was cooled down in an oven to 150 °C, then in a desiccator with $CaCl_2$ to room temperature and weighed. The arithmetic mean of the test results of two samples of each composition was taken as the final result.

3. Results and Discussion

3.1. Charge mixture XRD

The results of the charge mixture XRD after mechanochemical activation are shown in Fig. 2. For clarity, the XRD patterns are presented in the scan range 2Θ = 5–50°.

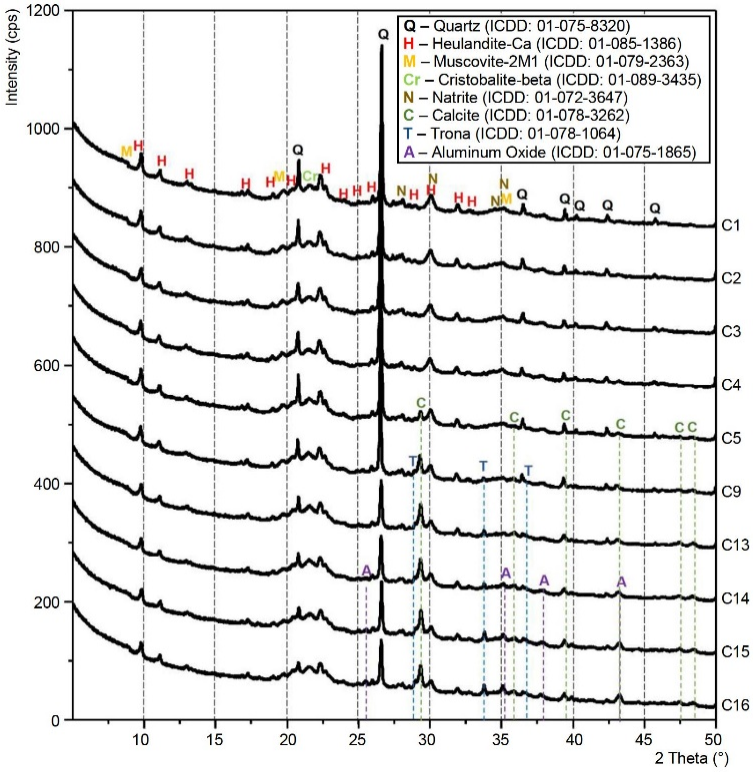

Figure 2. Charge mixture XRD patterns.

Based on the results of the XRD of the charge mixture samples (Fig. 2), the following was found out. The crystalline phase of the C1–C4 samples is represented (in addition to the data in Table 2) by the mineral natrite [Na_2CO_3, ICDD: 01-072-3647]. X-ray patterns of samples C5, C9, C13–C16 additionally showed peaks of the calcite's phase [$CaCO_3$, ICCD: 01-078-3262]. This phase is part of the R2 rock. The intensity of the lines increased with the increase in the amount of R2 rock in the charge mixture composition. In samples C9, C13–C16, additionally, there is a new phase of trona [$Na_3H(CO_3)_2(H_2O)_2$, ICDD: 01-078-1064], and in samples C14–C16 – aluminum oxide [Al_2O_3, ICDD: 01-075-1865].

X-ray patterns of samples C1–C4 and C5 show a wide halo in the region of 33–39° (2θ), which corresponds to the amorphous (nanocrystalline) phase. The effect may be attributed to sodium silicate hydrates. The formation of these compounds in a siliceous charge mixture after mechanochemical activation is described in the scholarly literature [24]. The intensity of the halo decreases with the increase in the amount of calcite and aluminum oxide in the charge mixture (Samples C5, C9, C13–C16). At the same time, the intensity of the natrite peaks decreases and the number of tronas in the samples increases. There is evidence in the scholarly literature for the formation of trona in the siliceous charge mixture after alkaline activation [24].

3.2. Charge mixture TA

By employing differential thermal analysis (DTA) and differential thermogravimetry (DTG), phase transformations in the charge mixture during heating were examined. The results are shown in Fig. 3.

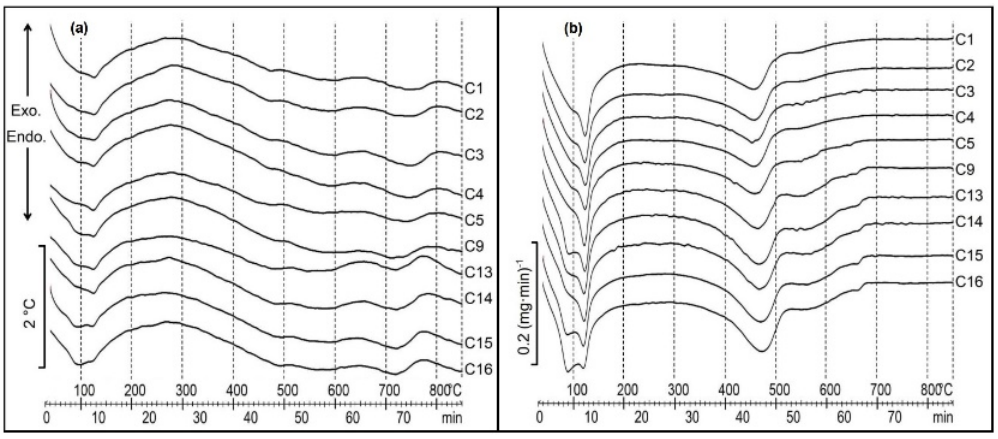

Figure 3. DTA (a) and DTG (b) curves of charge mixture samples.

Results of experimental analysis (Fig. 3) allow us to estimate the phase transformations in the charge mixture during heating. The first endothermic effect (Fig. 3a) and mass loss (Fig. 3b) in the temperature range from 80 to 110 °C confirm the XRD findings. The effect reflects the increase in the amount of trona in the charge mixture in response to the increase of calcite and simultaneously $CaCO_3$ and Al_2O_3 (Samples C9, C13–C16) in its composition.

The endothermic effect (Fig. 3a) with a peak at a temperature of ≈ 120 °C is associated with the release of water from sodium silicate hydrates. The effect is accompanied by weight loss (Fig. 3b). The formation of sodium silicate hydrates caused by mechanochemical activation of a siliceous charge mixture is considered in the article [24]. The intensity of the thermal effect and the rate of weight loss at a temperature of ≈ 120 °C decreases with the increase of $CaCO_3$ and simultaneously $CaCO_3$ and Al_2O_3 in the charge mixture (Samples C9, C13–C16). It can be assumed that this is due to the decrease in the amount of reaction active SiO_2 in the charge mixture. The decrease in the amount of trona and increase in sodium silicate hydrates in the charge mixture composition with a high CaO content is described in [30]. The effect occurred after intensive and lasting mechanochemical activation of the charge mixture, which facilitates the formation of reaction active SiO_2.

The following endothermic effect is reflected by DTA curves (Fig. 3a) in the temperature range from 300 to 510 °C. The effect is accompanied by a large loss of sample weight reflected by the DTG curves (Fig. 3b). In the siliceous charge mixture, sodium silicates are intensively formed in this temperature range. The findings are confirmed by the results in [24]. A large loss of mass is related with the decarbonization of sodium carbonate. The peak of the effect is slightly shifted to the region of high temperatures because of the increase of $CaCO_3$ and Al_2O_3 (Samples C1–C16) in the charge mixture composition.

The endoeffect and the insignificant rate of samples weight loss (C1–C4) in the temperature range from 510 to 650 °C are caused by the release of water vapor during condensation of OH groups. Many authors have observed a similar effect when annealing zeolite-containing rocks activated with alkaline solutions [18, 22, 24]. In this temperature range, surface hydroxyl groups (Si–O–H) are sealed in micropores [22, 24]. DTG curves of samples with calcite in the composition (C5–C16) in the temperature range from 510 to 620 °C, show that the rate of mass loss increases (Fig. 3b). The effect is additionally related with calcite decarbonization.

Insignificant endothermic effect and loss of samples weight at temperatures from 650 to 670 °C is related with decarbonization of unreacted $CaCO_3$. The effect has not been reflected by DTG curves on samples without calcite (C1–C4). Based on the results of experimental analysis (Fig. 3), the exposure temperature for obtaining samples of porous glass ceramics with a uniform pore structure (670 °C) was determined. The required exposure time is established experimentally.

The melting of the charge mixture begins at a temperature of > 680 °C. An endothermic effect is observed (Fig. 3a). The effect is that samples retain their mass. DTG curves in this temperature range (Fig. 3b) show straight lines. The effect of $CaCO_3$ and Al_2O_3 on the initial melting temperature of the charge is insignificant. The maximum of softening effect of the charge mixture shifts to the region of lower temperatures if there is increase in calcite in the rock. The shift of the peak of the endothermic effect from ≈ 750 °C for sample C1 (0 % calcite) to ≈ 720 °C for sample C13 (10.5 % calcite) was found. When Aluminum Oxide was introduced into the charge mixture composition, no change in the peak of the temperature effect was found. The appearance of a molten in the siliceous charge mixture in this temperature range was mentioned by other authors [17–19]. During the melting of the charge mixture, the free OH groups in the micropores condense and are released as water vapor [22, 24]. The charge mixture foams. The porosity of the glass ceramic material depends on the amount and viscosity of the molten in the charge mixture and the volume of gas released at a particular time. In this work, these properties were regulated by the heating rate of the charge mixture. The heating rate of the charge mixture – 4.5 °C/ min was determined experimentally.

The results of experimental analysis (Fig. 3) allow to estimate the crystallization temperature of the charge mixture. The crystallization of the siliceous charge mixture without calcite is characterized by a wide peak (exothermic effect) reflected by the DTA curve (Fig. 3a). The peak maximum at a temperature of ≈ 800 °C. The effect does not change when Al_2O_3 is introduced into the charge mixture in the amount of ≤ 3.05 %. The exothermic effect of crystallization shifts to the region of lower temperatures in response to the increase of calcite in the charge mixture composition. The peak maximum shifts to a temperature of ≈ 770 °C when heating a siliceous charge mixture with a calcite content equal to 10.5 % (Sample C13, Fig. 3a). The peak is obvious and more intensive in comparison with compositions without calcite (C1–C4). The effect of Al_2O_3 in the amount of ≤ 12.21 % on the crystallization of the siliceous charge mixture with calcite (10.5 %) is insignificant (Samples C13–C16). The intensity and temperature of the peak maximum remain almost unchanged.

3.3. Porous glass ceramics' XRD

X-ray pattern of samples of porous glass ceramic materials are shown in Fig. 4. For visual clarity, patterns are presented in the scan range 2Θ = 10–45°.

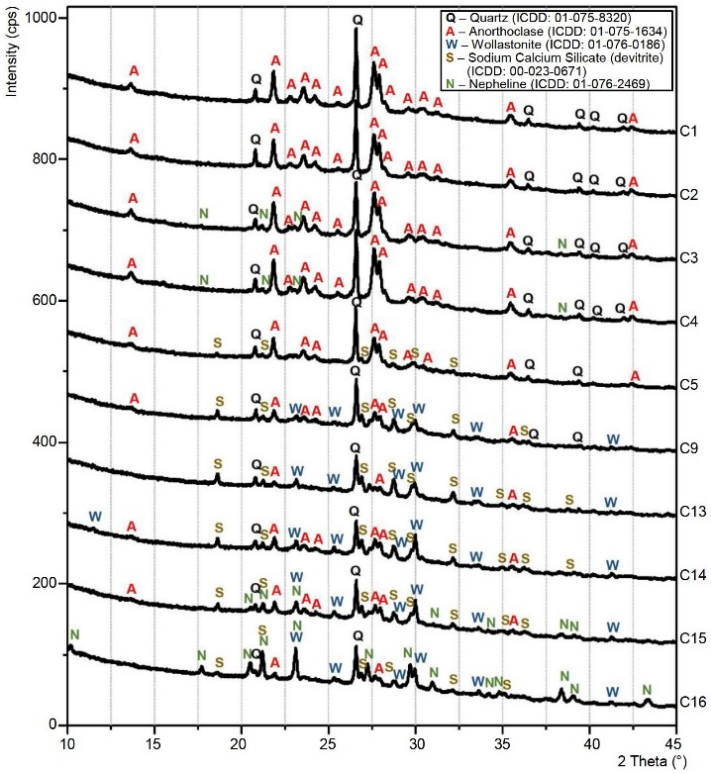

Figure 4. X-ray patterns of glass ceramic samples.

Based on the XRD results of glass ceramic samples (Fig. 4), the following has been established. On all X-ray patterns (Fig. 4), in the scan range from 17 to 37° (2θ), there is a non-monotonic change in the background (halo), probably caused by the presence of an amorphous phase. The change of the amorphous halo depending on the amount of CaO and Al_2O_3 in the composition of the material has not been detected. The main crystalline phases of C1–C4 samples are anorthoclase [$(Na_{0.85}K_{0.14})(AlSi_3O_8)$, ICDD: 01-075-1634] and quartz [SiO_2, ICDD: 01-075-8320]. The samples were obtained from a charge without calcite in the composition. After increasing the amount of Al_2O_3 additive in the charge mixture to 2.04 % or 3.05 %, the nepheline's phase additionally appeared in glass ceramics [$Na_3K(Si_{0.553}Al_{0.447})_8O_{16}$, ICDD: 01-076-2469]. The amount of new phase is insignificant. It is known from the scholarly literature that in porous glass ceramics made of zeolite tuff plagioclase may be present instead of anorthoclase [18, 24].

With the increase of the calcite in charge mixture, the intensity of the anorthoclase lines decreased. New lines appeared on X-ray patterns. The lines correspond to the crystalline phases of wollastonite [$CaSiO_3$, CDD: 01-076-0186] and sodium calcium silicate (devitrite) [$Na_2Ca_3Si_6O_{16}$, ICDD: 00-023-0671]. The intensities of the lines of the new phases increased in response to the increase of $CaCO_3$ in the rock composition to 10.5 % (Fig. 4, C5, C9, C13). The results obtained are consistent with the previously obtained research findings [22].

X-ray patterns of C13–C16 were obtained on samples from siliceous rock with calcite amount equal to 10.5 %. When amount of Al_2O_3 in the charge mixture was increased to 8.14 %, the intensity of the devitrite lines decreased, and those of wollastonite and anorthoclase increased. The nepheline lines appeared on the X-ray patterns. Further increase in the concentration of Al_2O_3 to 12.21 % caused the decrease in the amount of wollastonite in the composition, and the anorthoclase and devitrite lines practically disappeared. Nepheline has become the main crystalline phase of glass ceramics. The formation of the nepheline's phase in glass ceramics caused by the increased amount of Al_2O_3 in the composition of the material was also observed by other researchers [31].

3.4. Porous glass ceramics macrostructure

A scan of the surface of porous glass ceramic samples is shown in Fig. 5.

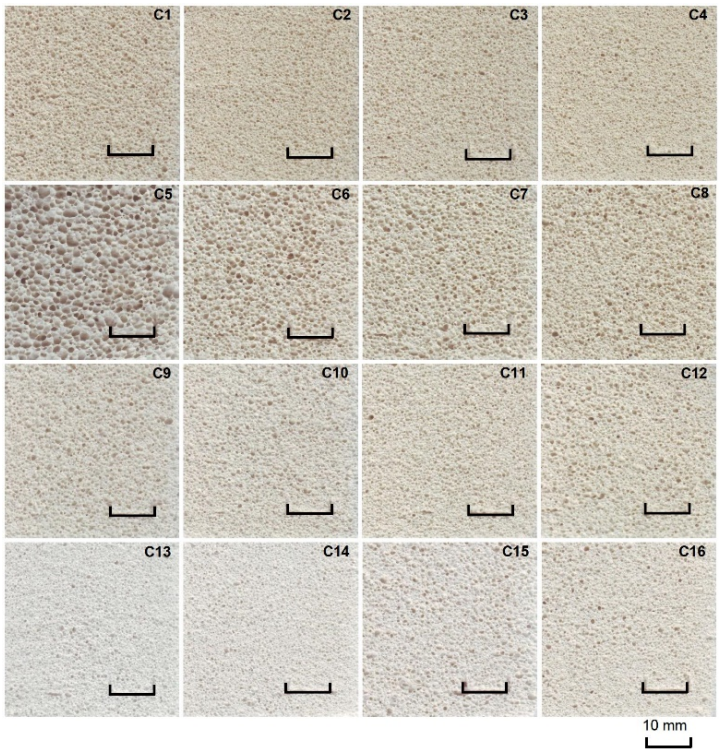

Figure 5. A scan of the surface of porous glass ceramic samples.

All samples of porous glass ceramic materials have a cellular (finely porous) structure (Fig. 5.). The porosity over the entire surface area of the samples is uniform. The pore size does not exceed 1.5 mm (except for samples C5). The maximum pore size in samples C5 ≈ 4 mm. With the increase of calcite in the charge mixture composition, the surface color of the annealed samples becomes lighter. And vice versa, it darkens with the increase of Al_2O_3. The different color of the surface can be attributed to a change in the phase composition of the samples. According to Fig. 4, the crystalline phase of light samples consists mainly of wollastonite and devitrite, and dark ones – anorthoclase, quartz and nepheline. The color of the samples surface can also be affected by the pore structure [8]. The results of the study into the microstructure of the samples are given below.

3.5. SEM images of samples

The effect of calcite in the charge composition on the microstructure of porous glass ceramics samples is shown in Fig. 6. The results were obtained by using the SEM. Samples of compositions C1, C9 and C13 were exposed to testing.

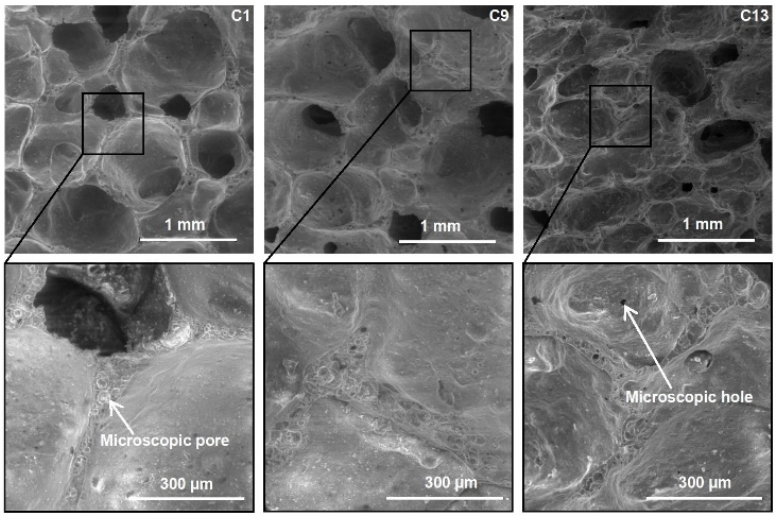

Figure 6. SEM images of samples.

The SEM images of sample C1 (Fig. 6) show pores with a diameter of ≤ 1 mm. The pores are in the shape of a ball, closed. Some of them are connected to each other. There are many closed micropores with a diameter of < 30 µm in the pore walls. The surface of the walls is smooth. The sample was obtained

from a calcite-free rock. The SEM images of sample C9 display pores with a diameter of < 1.5 mm. The shape is stretched. The individual pores are connected to each other by wide channels. The pore walls consist of closed micropores. Sample C9 was obtained from a rock containing 7 % of calcite. The pores in sample C13 have different diameters and shapes. Pore diameter is < 1 mm. The surface of the walls is uneven. There is a great deal of through microscopic holes with a diameter of < 30 μm between the pores. There are many closed and open micropores with a diameter of < 20 μm in the walls of large pores. It is known that open pores in glass ceramics are formed during intensive crystallization [6]. According to Fig. 3, with the increase of calcite content in siliceous rock up to 10.5 % (Sample C13), crystallization in glass ceramics begins at a lower temperature (≈ 770 °C). The exothermic effect of crystallization is more intense in comparison with the calcite-free composition. As a result, more open pores appear.

3.6. Micro-CT of samples

To study the macro- and microstructure inside porous glass ceramics, a Micro-CT of samples was carried out. Samples C1, C9 and C13 were tested. The samples were obtained from rocks with different calcite content. The test results are shown in Fig. 7.

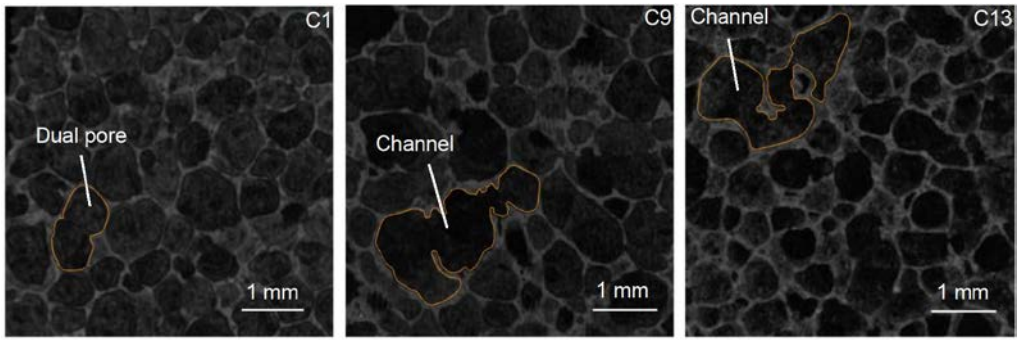

Figure 7. Micro-CT of samples.

The results of the Micro-CT samples (Fig. 7.) complement the SEM findings. The Micro-CT image inside the sample C1 shows pores with a diameter of < 1 mm. Some adjacent pores are merged. With the increase of calcite in the siliceous rock composition to 7 % (Sample C9), the number of merged pores increased. The image of C9 clearly shows a channel that connects more than 3 adjacent pores in one section of the sample. The diameter of select pores increased to 1.5 mm. With the 10.5 % calcite in the composition (Sample C 13), the length of channels in porous glass ceramics increased. The image of C13 shows a channel that connects more than 5 adjacent pores in one section of the sample. There are no ruptured walls inside the channel. The diameter of the pores decreased to 1mm or less. There are many bright dots in the walls of the pores. This indicates a large number of micropores in the sample.

Based on the analysis of the SEM and Micro-CT images, it was found that the macro- and microstructure of porous glass ceramics from siliceous rocks is significantly influenced by the amount of calcite in the charge mixture. The increase of $CaCO_3$ changes the size and shape of pores. Channels are formed inside the material, which consist of connected adjacent pores. Microscopic holes appear in the pores' walls.

3.7. Samples' density and porosity

Fig. 8 shows dependency graphs of the apparent density and porosity of glass ceramic samples on the amount of $CaCO_3$ and Al_2O_3 in the charge mixture composition.

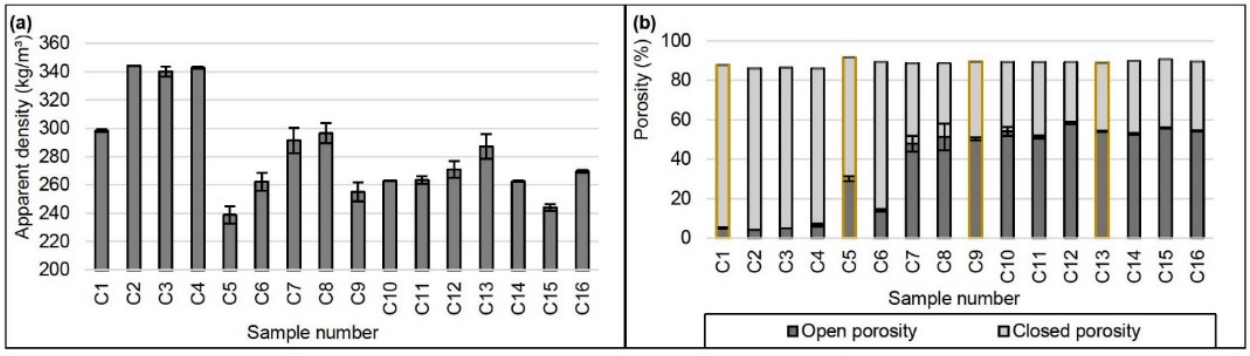

Figure 8. Apparent density (a) and porosity (b) of samples.

The effect of calcite in the siliceous rock composition on the apparent density of porous glass ceramic samples is as follows (Fig. 8a, samples C1, C5, C9, C13). The apparent density of the samples decreased from ≈ 300 kg/m^3 to ≈ 240 kg/m^3 in response to a 3.5 % increase of $CaCO_3$ in the rock. A further increase of calcite in the rock to 10.5 %, increased the apparent density of the samples linearly to ≈ 285 kg/m^3 (Sample C13). The obtained dependencies are similar to the findings of other authors. The effect of CaO on the apparent density of samples of porous glass ceramics from fly ash is similar [26, 27].

Dependences of changes in the samples' apparent density on the amount of Al_2O_3 additive have been obtained. Depending on the amount of calcite in the rock, the addition of Al_2O_3 affects the apparent density of glass ceramics in different ways. The samples density increased if $CaCO_3$ content in the rock amounted to ≤ 3.5 % and the introduction of Al_2O_3 additive was up to 6.11 % (Samples C1–C8). The addition of Al_2O_3 in an amount of ≤ 8.14 % caused the decrease in the apparent density of samples from ≈ 285 kg/m^3 to ≈ 244 kg/m^3 with a 10.5 % calcite content in the rock (Samples C13–C15). The increase of Al_2O_3 additive to more than 8.14 % in the charge mixture raised the apparent density of the samples (Sample C16).

Based on the findings obtained (Fig. 8b), the total porosity of the samples of glass ceramic materials is in the range from 85.70 to 91.54 %. The lowest values of the total porosity demonstrate the samples from the calcite-free charge mixture (C1–C4). In given samples > 79 % of the pores are closed. It is easy to trace the characteristic dependence between the increase in the number of open pores in the material and the increase in the amount of calcite in the charge mixture composition. For sample C13, the open porosity is > 54 %. The addition of Al_2O_3 also increases the number of open pores in the material. The findings obtained confirm the results of TA, SEM and Micro-CT.

3.8. Strength

Fig. 9 shows the strength values of porous glass ceramic samples from siliceous rocks.

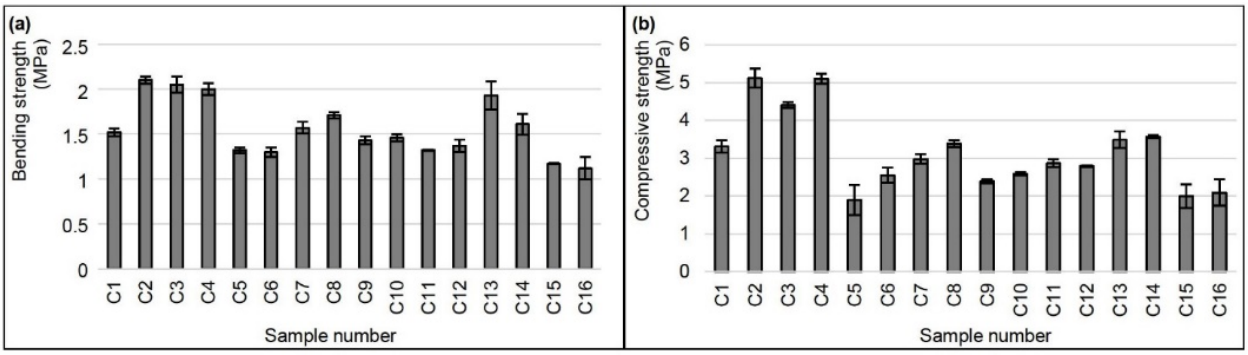

Figure 9. Bending (a) and compressive strength (b) of samples.

According to the conducted research (Fig. 9), the obtained porous glass ceramic materials have a bending strength in the range from 1.12 to 2.1 MPa. The compressive strength is in the range of 1.9–5.1 MPa. The following relationship is traced between the phase composition of the material and the bending strength of the samples (Fig. 9a). With the increase of the wollastonite mineral in the material, the bending strength increased. Thus, for samples C9, bending strength ≈ 1.5 MPa. The strength is similar for samples of composition C1. However, the average density of samples C1 is 40 kg/m^3 higher than that of samples C9. The bending strength of samples C13 is 1.93 MPa at a density ≈ 285 kg/m^3. The value is commensurate with the test results of samples C4, which density is ≈ 340 kg/m^3. There is evidence in the scholarly literature on the positive effect of the wollastonite mineral on the bending strength of glass ceramic materials [32].

The negative influence of the mineral nepheline in porous glass ceramics samples on their bending strength has been revealed. The crystalline phase of sample C16 consists mainly of this mineral. The samples have the lowest bending strength (1.12 MPa). The effect of the Al_2O_3 content in the composition of glass ceramics on its strength characteristics has been explored in the works of other authors [28, 29]. The authors have established the maximum concentration of aluminum oxide in the composition of glass ceramics.

According to the research findings (Fig. 9b), the compressive strength of samples of porous glass ceramic materials is linearly related to the apparent density. The highest compressive strength (≈ 5 MPa) was in samples C2 and C4. The apparent density of samples is slightly more than 340 kg/m^3. The lowest compressive strength of samples C5, C15, C16 (≈ 2 MPa). Samples of compositions C5, C15 have the lowest density (≈ 240 kg/m^3). Probably, the samples C16 are less durable due to the nepheline content. According to Fig. 4, the main crystalline phase of the sample is nepheline. It was not possible to find other

relationships between the phase composition and compressive strength of the samples. The obtained porous glass ceramics with an equal apparent density are superior in strength to foam glass and glass ceramics from industrial waste [1, 7, 11–16].

3.9. Thermal conductivity

Fig. 10 shows the results of thermal conductivity testing of porous glass ceramic samples. The results are shown in relation to the apparent density of the samples.

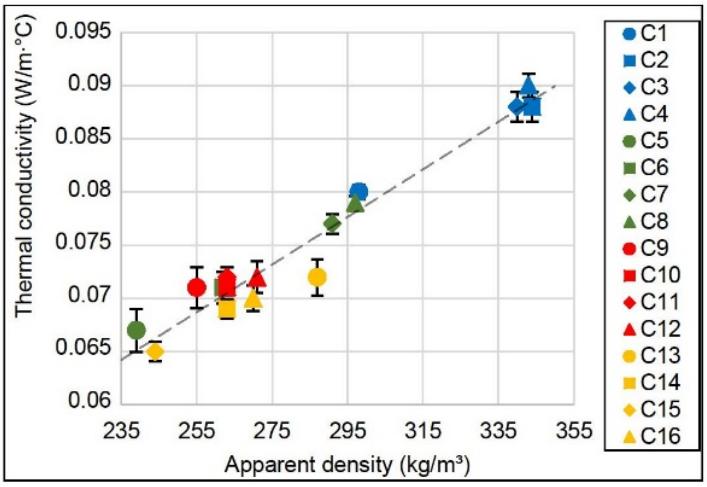

Figure 10. Thermal conductivity of samples.

The findings presented in Fig. 9 underwent a thorough analysis. The dependence of the thermal conductivity of porous glass ceramic samples on their apparent density was established. The dependence is linear. It refers to samples with a density from 235 to 355 kg/m³. The dependence of thermal conductivity on the density of samples is expressed by the formula (6):

$$\lambda = 21.7 \cdot 10^{-5} \cdot \rho + 0.014, \quad (6)$$

where λ is thermal conductivity (W/(m·°C)); ρ is apparent density of the material dry basis (kg/m³).

The validity coefficient of the approximation $\left(R^2\right)$ is equal to 0.971.

The thermal conductivity values of all samples from siliceous rock with a 10.5 % calcite (C13–C16) are below the regression line (Fig. 9). It is known that thermal conductivity depends largely on the conductivity in the solid phase [6]. According to the SEM and Micro-CT findings, the increase in the amount of $CaCO_3$ in the charge mixture raised the number of micropores in the pore walls of the samples. Probably, owing to this, the thermal conductivity of porous glass ceramics has decreased.

Following the results of the experiment, it was found that dry samples C15 of porous glass ceramics have the lowest thermal conductivity (0.065 W/(m·°C)). The apparent density of the samples is 244 kg/m³. Highest thermal conductivity (0.09 W/(m·°C)) belongs to samples of composition C3 (apparent density is 340 kg/m³). The influence of the phase composition of samples of porous glass ceramic materials on their thermal conductivity has not been revealed. The results obtained correlate with the findings supplied by other authors [6].

3.10. Limiting operating temperature

The main goal of our work is to obtain porous glass ceramic materials with an operating temperature of more than 900 °C. The effect of the phase composition of porous glass ceramics on the limiting operating temperature of materials is shown in Fig. 11. The limiting temperature was estimated by the size of the samples after holding for 2 hours at a given temperature.

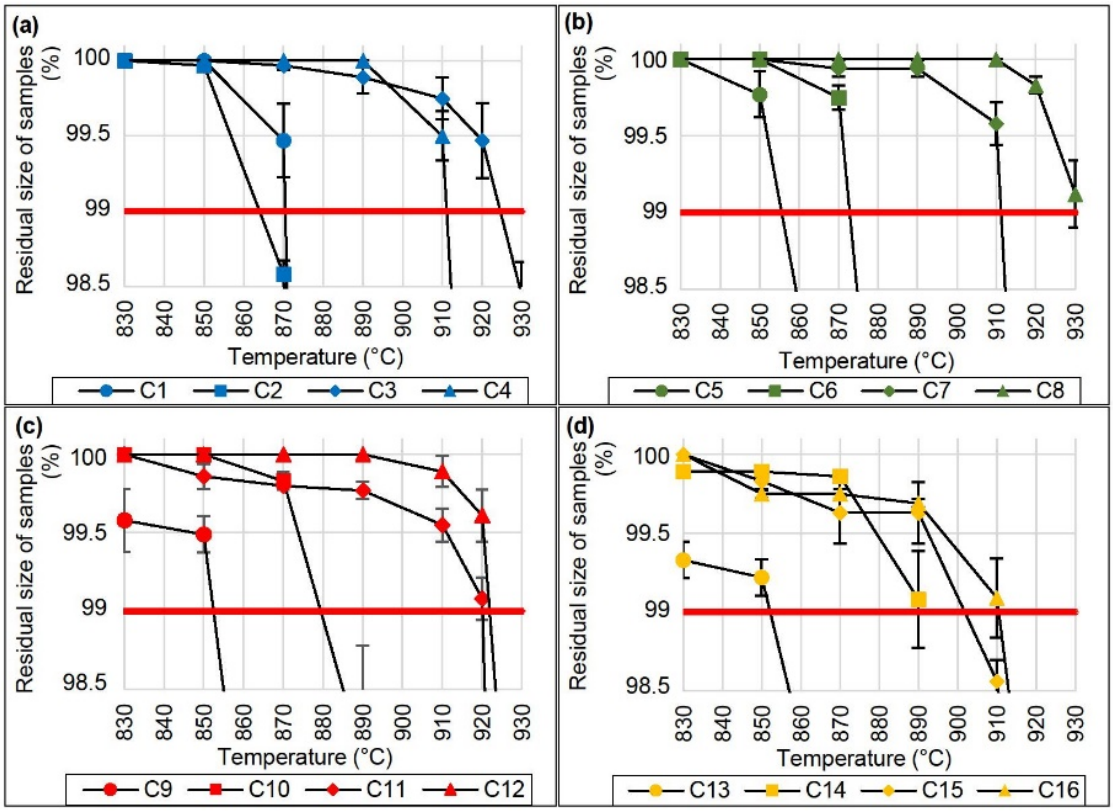

Figure 11. Residual size of samples after holding for 2 hours at a given temperature. (Samples from siliceous rock with calcite content equal to: a – 0%, b – 3,5%; c – 7%; d – 10,5%; C1–C16 – numbers of compositions)

During the experiment, it was found that the compositions C3, C4, C7, C8, C11, C12, C16 can be operated at a temperature > 900 °C. The residual sizes of the samples after holding for 2 hours at a temperature of more than 900 °C are larger than 99 % of the control values (Fig. 11). All compositions were obtained by modifying the charge mixture with aluminum oxide. The positive effect of Al_2O_3 in the composition of ceramic materials on their resistance to a lasting exposure to high temperatures have been explored in the scholarly literature [28, 29]. Following the analysis of findings in Fig.11 we have found that the amount of Al_2O_3 additive must be adjusted depending on the amount of calcite in the charge mixture. The amount of Al_2O_3 must be increased with reference to $CaCO_3$ increase. To achieve the limiting operating temperature of porous glass ceramics > 900 °C is possible if we modify the charge mixture with a 2.04 % or more Al_2O_3. Calcite-free charge mixture (Samples C3, C4). The phase composition of the samples consists of anorthoclase, nepheline and quartz (Fig. 4). With a 10.5 % amount of calcite in the rock, it was also possible to obtain glass ceramics with an operating temperature > 900 °C. The amount of Al_2O_3 in the charge should be equal 12.21 % (Sample C16). According to Fig. 4, the main crystalline phase of the samples is anorthoclase, nepheline, quartz and wollastonite.

Samples C5, C9, C13 can be operated at a temperature of no more than 850 °C. The crystal phase of these samples contains a lot of devitrite. This compound has a low melting point [33]. The effect of devitrite on the limiting operating temperature is negative.

The developed porous glass ceramic materials significantly exceed foam glass and porous glass ceramics from siliceous rocks based on charge mixture exposed to alkaline activation in terms of the limiting operating temperature [17–19]. The glass-ceramic materials from siliceous rock can be used as thermal insulation of melting furnaces, boiler equipment, etc.

3.11. Thermal shock resistance

Thermal insulation materials used in the insulation of industrial equipment should have high thermal shock resistance [2, 28, 29]. Thermal shock resistance is the ability of material not to break down when exposed to sudden temperature changes. Fig. 12 shows the results of testing the thermal shock resistance of porous glass ceramic samples.

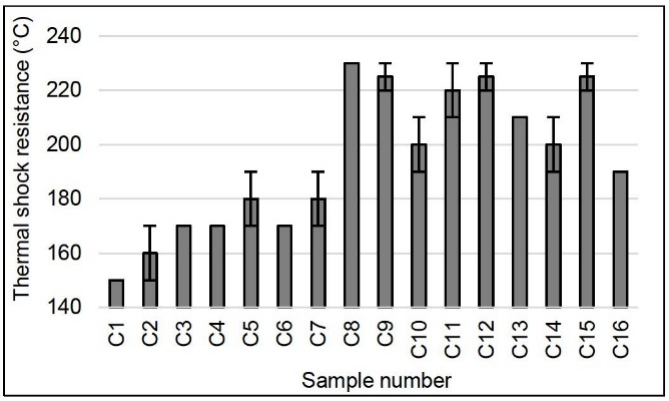

Figure 12. Thermal shock resistance.

Based on obtained findings (Fig. 12), the thermal shock resistance of porous glass ceramic samples varies depending on the composition. The lowest values of thermal shock resistance have samples from the calcite-free charge mixture. The values are in the range of 150–170 °C. Owing to the increase of the aluminum oxide in the charge mixture composition to 2.04 % or more, a linear increase in the thermal shock resistance of the samples from 150 to 170 °C occurs. There is a linear relationship between the values of thermal shock resistance of samples of glass-ceramic materials and their porosity. The more closed pores in the material, the less stability. The thermal shock resistance of samples C1–C4 and C6 does not exceed 170 °C. More than 75 % of the pores in these samples are closed (Fig. 8b). During the experiment, heated samples were immersed in water. Owing to the pores' structure, water did not penetrate into the material. The sample surface cooled faster. The sample was destroying due to the large temperature difference on the surface and inside of it. Consequently, the increase in the number of open pores in the material raised the thermal shock resistance of the samples. Maximum thermal shock resistance (225–230 °C) belongs to the samples C8, C9, C12 and C15. The number of open pores in the material is > 50 % (Fig. 8b). The assumption about the relationship between thermal shock resistance and porosity of the material is confirmed. Similar conclusions can be found in [6].

After analyzing the values in Fig. 12, the negative effect of nepheline on the thermal shock resistance of the samples was established. Sample C16 failed at a temperature drop of 190 °C. This is 35 °C less in comparison with the sample C15. According to Fig. 8b, the number of open pores in both samples is almost equal (> 54 %). The main difference is in the phase composition. There is more nepheline in the sample C16.

The thermal shock resistance of the developed porous glass ceramic materials is almost equal to that of foam glass and porous glass ceramics derived from industrial waste [28, 29].

3.12. Chemical stability

The influence of the chemical and mineralogical composition of porous glass ceramic materials on the chemical stability of samples is shown in Table 4. Chemical stability was determined by the loss of weight of powdered samples (fraction 0.315–0.63 mm) after boiling for 3 hours in aggressive chemical media.

Table 4. Change in the samples' weight after boiling in chemical media for 3 hours.

Sample number	Change in the samples' weight after boiling in chemical media for 3 hours (%)*		
	H_2O	6N HCl solution	1N Na_2CO_3 solution + 1N NaOH solution (1:1)
C1	0.82	1.37	6.95
C2	0.17	0.63	6.75
C3	0.67	1.47	7.05
C4	0.37	1.10	7.12
C5	0.39	0.59	6.93
C6	0.34	1.60	7.31
C7	0.54	1.99	6.71
C8	0.63	2.20	6.68
C9	0.47	1.91	7.17
C10	0.41	3.13	7.20

Sample number	Change in the samples' weight after boiling in chemical media for 3 hours (%)*		
	H_2O	6N HCl solution	1N Na_2CO_3 solution + 1N NaOH solution (1:1)
C11	0.97	4.44	6.80
C12	0.56	7.13	6.69
C13	0.99	4.80	7.94
C14	0.57	5.42	7.45
C15	0.73	7.81	7.46
C16	0.56	17.89	6.99

** – The differences in the test results of the samples of each composition did not exceed 5% of the average value.*

After the analysis of the experimental findings (Table 4), the following ensues. After boiling samples of glass ceramic materials (fraction 0.315–0.63 mm) for 3 hours in water, all samples lost less than 1 % in weight. This result confirms the ability of glass ceramic materials not to be destroyed by the action of water. The material can be operated in wet conditions without restrictions.

The influence of the phase composition of glass ceramic samples on their chemical stability in an aqueous solution of HCl (6N) has been established. The stability decreases in response to the increase in the amount of wollastonite, devitrite and nepheline in the material. After 3 hours of boiling the sample C16, the color of the solution turned bright yellow. The sample weight decreased by 17.89 %. Sample C16 contains the largest amount of wollastonite and nepheline (Fig. 4). Samples in which the main crystalline phase is anorthoclase and quartz (C1–C5) are almost unsusceptible to chemical corrosion in an aqueous solution of HCl (6N). The mass loss does not exceed 1.5 %. There is a great deal of evidence in the scholarly literature on the dissolution of nepheline and wollastonite minerals in aqueous solutions of hydrochloric acid [34].

The effect of the phase composition of glass-ceramic samples on the resistance to alkaline solutions (Na_2CO_3 (1N) + NaOH (1N)) has not been detected. The chemical stability of the samples deteriorates slightly after the increase of CaO in their compositions. The weight loss increased from 6.95 % (Sample C1) to 7.94 % (Sample C13). There is evidence in the scholarly literature about the negative effect of CaO in the composition of glass ceramics on its chemical stability [35]. The effect of addition of Al_2O_3 in the amount of up to 12.21 % to the charge mixture composition on the resistance of glass ceramic samples in alkalis is insignificant.

The completed experimental studies of samples of glass ceramic materials allowed to reveal their high chemical stability in water, HCl aqueous solution and alkalis. With reference to some indicators, porous glass-ceramic materials from siliceous rocks surpassed foam glass [35]. It is recommended to use the developed materials as insulation for pipelines, industrial installations, etc.

4. Conclusions

Porous glass-ceramic materials were obtained from siliceous rocks with different amounts of calcite in their composition. To raise the limiting operating temperature of the samples, aluminum oxide was added to the charge mixture. A joint mechanochemical activation of components (siliceous rocks, Na_2CO_3, Al_2O_3 and KCl) was carried out in a planetary ball mill. The resulting charge was annealed at a temperature of 850 °C. The influence of the calcite and aluminum oxide content in the charge mixture composition on the properties of porous glass-ceramics samples has been revealed.

Main conclusions:

- The main crystalline phase of glass ceramics from a calcite-free charge mixture is anorthoclase and quartz. The calcite-containing charge mixture samples additionally contain wollastonite and devitrite. After increasing the amount of Al_2O_3 additive in the composition of the charge mixture, nepheline appears in glass ceramics. The influence of the phase composition of glass ceramics on the properties of samples has been examined.
- Glass-ceramic materials from siliceous rocks have a finely porous structure. The pore size of most samples is less than 1.5 mm. The increase in the calcite and aluminum oxide amount in the charge mixture composition had a significant impact on the glass ceramics microstructure. The size and shape of the pores have changed. The number of open pores in the material increased from ≈ 5 % to > 50 %.

- The developed porous glass ceramics has an apparent density of 239–344 kg/m^3, bending and compressive strength up to 2.1 MPa and 5.1 MPa, respectively.
- The developed porous glass ceramics has a thermal conductivity is 0.065–0.09 W/(m°·C), thermal shock resistance up to 230 °C, limiting operating temperature up to 920 °C. The limiting operating temperature of the samples was increased to 920 °C owing to the introduction of Al_2O_3 additive into the charge mixture. The amount of the additive depends on the amount of calcite in the siliceous rock. With the increase in the $CaCO_3$ amount it is necessary to increase Al_2O_3 content. The 10.5 % content of calcite in the siliceous rock allowed to obtain porous glass ceramics with an operating temperature over 900 °C. The additive of Al_2O_3 in the amount of > 8.14 % was dispensed into the charge mixture composition.
- The completed experimental studies of samples of glass ceramic materials allowed to reveal their high chemical stability in water, HCl aqueous solution and alkalis.
- Porous glass-ceramic materials from siliceous rocks are superior in many respects to foam glass and porous glass ceramics from industrial waste. This material can be used in the construction and repair of industrial and civil facilities (for heat and sound insulation, as a refractory lining of furnaces, for protection of structures from corrosion, etc.).

References

1. Fernandes, H.R., Tulyaganov, D.U., Ferreira, J.M.F. Preparation and characterization of foams from sheet glass and fly ash using carbonates as foaming agents. Ceramics International. 2009. 35 (1). Pp. 229–235. DOI: 10.1016/j.ceramint.2007.10.019
2. Guo, H., Ye, F., Li, W., Song, X., Xie, G. Preparation and characterization of foamed microporous mullite ceramics based on kyanite. Ceramics International. 2015. 41 (10). Pp. 14645–14651. DOI: 10.1016/j.ceramint.2015.07.186
3. Bessmertnyi, V.S., Lesovik, V.S., Krokhin, V.P., Puchka, O.V., Nikiforova E.P. The Reducing Effect of Argon in the Plasma Treatment of High-Melting Nonmetallic Materials (A Review). Glass and Ceramics. 2001. Vol. 58. Pp. 362–364. DOI: 10.1023/A:1013963916418
4. Jabir, H.A., Abid, S.R., Murali, G., Ali, S.H., Klyuev, S., Fediuk, R., Vatin, N., Promakhov, V., Vasilev, Y. Experimental Tests and Reliability Analysis of the Cracking Impact Resistance of UHPFRC. Fibers. 2020. 8 (12). Article No. 74. DOI: 10.3390/fib8120074
5. Smirnova, O.M., Potyomkin, D.A. Influence of ground granulated blast furnace slag properties on the superplasticizers effect. International Journal of Civil Engineering and Technology. 2018. 9 (7). Pp. 874–880.
6. König, J., Lopez-Gil, A., Cimavilla-Roman, P., Rodriguez-Perez, M.A., Petersen, R.R., Østergaard, M.B., Iversen, N., Yue, Y., Spreitzer, M. Synthesis and properties of open- and closed-porous foamed glass with a low density. Construction and Building Materials. 2020. Vol. 247. Article No. 118574. DOI: 10.1016/j.conbuildmat.2020.118574
7. Zhu, M., Ji, R., Li, Z., Wang, H., Liu, L., Zhang, Z. Preparation of glass ceramic foams for thermal insulation applications from coal fly ash and waste glass. Construction and Building Materials. 2016. Vol. 112. Pp. 398–405. DOI: 10.1016/j.conbuildmat.2016.02.183
8. Cao, J., Lu, J., Jiang, L., Wang, Z. Sinterability, microstructure and compressive strength of porous glass-ceramics from metallurgical silicon slag and waste glass. Ceramics International. 2016. 42 (8). Pp. 10079–10084. DOI: 10.1016/j.ceramint.2016.03.113
9. Kyaw Oo D'Amore, G., Caniato, M., Travan, A., Turco, G., Marsich, L., Ferluga, A., Schmid, C. Innovative thermal and acoustic insulation foam from recycled waste glass powder. Journal of Cleaner Production. 2017. Vol. 165. Pp. 1306–1315. DOI: 10.1016/j.jclepro.2017.07.214
10. Yatsenko, E.A., Ryabova, A.V., Goltsman, B.M. Development of fiber-glass composite coatings for protection of steel oil pipelines from internal and external corrosion. Chernye Metally. 2019. Vol. 12. Pp. 46–51.
11. Yatsenko, E.A., Gol'tsman, B.M., Kosarev, A.S., Karandashova, N.S., Smolii, V.A., Yatsenko, L.A. Synthesis of Foamed Glass Based on Slag and a Glycerol Pore-Forming Mixture. Glass Physics and Chemistry. 2018. 44 (2). Pp 152–155. DOI: 10.1134/S1087659618020177
12. Ji, R., Zheng, Y., Zou, Z., Chen, Z., Wei, S., Jin, X., Zhang, M. Utilization of mineral wool waste and waste glass for synthesis of foam glass at low temperature. Construction and Building Materials. 2019. Vol. 215. Pp. 623–632. DOI: 10.1016/j.conbuildmat.2019.04.226
13. Jia, R., Deng, L., Yun, F., Li, H., Zhang, X., Jia, X. Effects of SiO2/CaO ratio on viscosity, structure, and mechanical properties of blast furnace slag glass ceramics. Materials Chemistry and Physics. 2019. Vol. 233. Pp. 155–162. DOI: 10.1016/j.matchemphys.2019.05.065
14. Hisham, N.A.N., Zaid, M.H.M., Aziz, S.H.A., Muhammad, F.D. Comparison of foam glass-ceramics with different composition derived from ark clamshell (ACS) and soda lime silica (SLS) glass bottles sintered at various temperatures. Materials. 2021. 14(3). Article No. 570. DOI: 10.3390/ma14030570
15. Zeng, L., Sun, H., Peng, T., Zheng, W. Preparation of porous glass-ceramics from coal fly ash and asbestos tailings by high-temperature pore-forming. Waste Management. 2020. Vol. 106. Pp. 184–192. DOI: 10.1016/j.wasman.2020.03.008
16. Romero, A.R., Toniolo, N., Boccaccini, A.R., Bernardo, E. Glass-ceramic foams from 'weak alkali activation' and gel-casting of waste glass/fly ash mixtures. Materials. 2019. 12 (4). Article No. 588. DOI: 10.3390/ma12040588
17. Ivanov, K.S. Optimization of the structure and properties of foam-glass ceramics. Magazine of Civil Engineering. 2019. 89 (5). Pp. 52–60. DOI: 10.18720/MCE.89.5
18. Kazantseva, L.K., Rashchenko, S.V. Optimization of porous heat-insulating ceramics manufacturing from zeolitic rocks. Ceramics International. 2016. 42 (16). Pp. 19250–19256. DOI: 10.1016/j.ceramint.2016.09.091
19. Yatsenko, E.A., Goltsman, B.M., Klimova, L.V., Yatsenko, L.A. Peculiarities of foam glass synthesis from natural silica-containing raw materials. Journal of Thermal Analysis and Calorimetry. 2020. 142 (1). Pp. 119–127. DOI: 10.1007/s10973-020-10015-3

20. Zhimalov, A.A., Bondareva, L.N., Igitkhanyan, Y.G., Ivashchenko, Y.G. Use of Amorphous Siliceous Rocks – Opokas to Obtain Foam Glass with Low Foaming Temperature. Steklo i Keramika (Glass and Ceramics). 2017. 74 (1–2). Pp. 13–15. DOI: 10.1007/s10717-017-9916-1
21. Kruszewski, Ł., Palchik, V., Vapnik, Y., Nowak, K., Banasik, K., Galuskina, I. Mineralogical, geochemical, and rock mechanic characteristics of zeolite-bearing rocks of the hatrurim basin, Israel. Minerals. 2021. 11(10). Article No. 1062. DOI: 10.3390/min11101062
22. Erofeev, V., Rodin, A., Bochkin, V., Ermakov, A. The formation mechanism of the porous structure of glass ceramics from siliceous rock. Magazine of Civil Engineering. 2020. 100 (8). Article No.10006. DOI: 10.18720/MCE.100.6
23. Erofeev, V.T., Rodin, A.I., Bochkin, V.S., Ermakov, A.A. Properties of porous glass ceramics based on siliceous rocks. Magazine of Civil Engineering. 2021. 102 (2). Article No. 10202. DOI: 10.34910/MCE.102.2
24. Kazantseva, L.K., Rashchenko, S.V. Chemical processes during energy-saving preparation of lightweight ceramics. Journal of the American Ceramic Society. 2014. 97 (6). Pp. 1743–1749. DOI: 10.1111/jace.12980
25. Li, Y., Zhao, L.-H., Wang, Y.-K., Cang, D.-Q. Effects of Fe2O3 on the properties of ceramics from steel slag. International Journal of Minerals, Metallurgy and Materials. 2018. 25 (4). Pp. 413–419. DOI: 10.1007/s12613-018-1586-7
26. Zhou, M., Ge, X., Wang, H., Chen, L., Chen, X. Effect of the CaO content and decomposition of calcium-containing minerals on properties and microstructure of ceramic foams from fly ash. Ceramics International. 2017. 43 (12). Pp. 9451–9457. DOI: 10.1016/j.ceramint.2017.04.122
27. Liu, Z.B., Zong, Y.B., Ma, H.Y., Dai, W.B., Li, S.H. Effect of (CaO+MgO)/SiO_2 ratio on crystallisation and properties of slag glass-ceramics. Advances in Applied Ceramics. 2014. 113 (7). Pp. 411–418. DOI: 10.1179/1743676114Y.0000000187
28. Costa, F.P.D., Morais, C.R.D.S., Pinto, H.C., Rodrigues, A.M. Microstructure and physico-mechanical properties of Al_2O_3-doped sustainable glass-ceramic foams. Materials Chemistry and Physics. 2020. Vol. 256. Article No. 123612. DOI: 10.1016/j.matchemphys.2020.123612
29. 29. Keyvani, N., Marghussian, V.K., Rezaie, H.R., Kord, M. Effect of Al_2O_3 content on crystallization behavior, microstructure, and mechanical properties of SiO_2–Al_2O_3–CaO–MgO glass-ceramics. International Journal of Applied Ceramic Technology. 2011. 8(1). Pp. 203–213. DOI: 10.1111/j.1744-7402.2009.02428.x
30. Kazantseva, L.K., Lygina, T.Z., Rashchenko, S.V., Tsyplakov, D.S. Preparation of Sound-Insulating Lightweight Ceramics from Aluminosilicate Rocks with High CaCO3 Content. Journal of the American Ceramic Society. 2015. 98 (7). Pp. 2047–2051. DOI: 10.1111/jace.13581
31. McClane, D.L., Amoroso, J.W., Fox, K.M., Hsieh, M.C., Kesterson, M.R., Kruger, A.A. Nepheline crystallization and the residual glass composition: Understanding waste glass durability. International Journal of Applied Glass Science. 2020. 11 (4). Pp. 649–659. DOI: 10.1111/ijag.15418
32. Almasri, K.A., Sidek, H.A.A., Matori, K.A., Zaid, M.H.M. Effect of sintering temperature on physical, structural and optical properties of wollastonite based glass-ceramic derived from waste soda lime silica glasses. Results in Physics. 2017. Vol. 7. Pp. 2242–2247. DOI: 10.1016/j.rinp.2017.04.022
33. Yang, S., Lu, J.-X., Poon, C.S. Recycling of waste glass in cement mortars: Mechanical properties under high temperature loading. Resources Conservation and Recycling. 2021. Vol. 174. Article No. 105831. DOI: 10.1016/j.resconrec.2021.105831
34. Bagani, M., Balomenos, E., Panias, D. Nepheline Syenite as an Alternative Source for Aluminum Production. Minerals. 2021. 11 (7). Article No. 734. DOI: 10.3390/min11070734
35. Abdel-Hameed, S.A.M., El-kheshen, A.A. Thermal and chemical properties of diopside-wollastonite glass-ceramics in the SiO_2–CaO–MgO system from raw materials. Ceramics International. 2013. 29(3). Pp. 265–269. DOI: 10.1016/S0272-8842(02)00114-1

Information about authors:

***Alexander Rodin**, PhD in Technical Science*
ORCID: https://orcid.org/0000-0002-8080-9808
E-mail: al_rodin@mail.ru

***Anatolij Ermakov**,*
ORCID: https://orcid.org/0000-0002-2560-0948
E-mail: anatoly.ermakov97@mail.ru

***Vladimir Kyashkin**, PhD in Physical and Mathematical Science*
ORCID: https://orcid.org/0000-0002-3413-247X
E-mail: kyashkin@mail.ru

***Natalya Rodina**,*
ORCID: https://orcid.org/0000-0002-4709-4847
E-mail: rodina.ng@list.ru

***Vladimir Erofeev**, Doctor of Technical Science*
ORCID: https://orcid.org/0000-0001-8407-8144
E-mail: yerofeevvt@mail.ru

Received 20.04.2022. Approved after reviewing 06.05.2022. Accepted 11.05.2022.